2015 International Conference on Unmanned Aircraft Systems (ICUAS)
Denver Marriott Tech Center
Denver, Colorado, USA, June 9-12, 2015

Tracking Multiple Mobile Targets Using Cooperative Unmanned Aerial Vehicles

Negar Farmani[1], Liang Sun and Daniel Pack

Abstract— **In this paper, we present a decentralized cooperative multiple target tracking method for multiple Unmanned Aerial Vehicles (UAVs). The decentralized cooperative multi-target tracking algorithm incorporates an optimal sensor management scheme and a cooperative path planner. To localize and track targets, a set of Extended Kalman Filters (EKFs) is used onboard each UAV and resulting target estimates are shared among UAVs. The sensor management scheme determines optimal gimbal poses to track the maximum number of targets using a greedy algorithm and a path planner is used to coordinate desired trajectories of UAVs. The effectiveness of the proposed algorithm is demonstrated using simulation results.**

I. INTRODUCTION

The applications of multiple UAVs have been widely reported in recent years. A team of cooperative UAVs, equipped with vision sensors and communication modules, can engage in search and rescue missions, map an unknown area, and perform natural disaster assessments. Such UAVs, activating as a mobile sensor network, can also collect real-time data in dynamic and complex environments. To that end, a real-time distributed decision making method to cooperatively maximize the control, sensing, and communication capabilities is a necessity. This paper presents one such method for multiple UAVs to autonomously track and locate multiple targets.

In a centralized system, all sensor measurements are collected to make optimal decisions, an unrealistic scenario in an environment with a large number of UAVs and targets. In a decentralized system, we sacrifice the optimal solutions for a scalable system. In our system, each UAV processes the sensor data independently and makes both control and sensing decisions for itself based on its observations of the environment and information communicated by neighboring UAVs. The overall challenge is to determine optimal task allocation based on the collective resources a group possesses.

Several researchers proposed distributed task allocation methods for multiple UAVs. Chen et al. [1] presented an algorithm based on the principles of genetic algorithm (GA). Simulation results show that the GA method provides an effective solution for the task allocation problem. Beruccelli et al. [2] showed the Consensus Based Bundle Algorithm (CBBA) to guarantee conflict-free multi-UAV path assignments. Darrah et al. [3] reported a dynamic task allocation technique for multiple UAVs using Mixed Integer Linear Programming (MILP). Tasks are assigned based on the number of mission vehicles and the number of targets that have been either detected or partially prosecuted. Sujit et al. [4] presented a negotiation scheme for multiple UAVs with limited sensor and communication ranges. They presented a negotiation method between neighbors to better exchange target information. Kim et al. [5] addressed the search planning and task allocation problem for a team of UAVs where each has different sensing and attack capabilities. They generated a search path for each UAV to detect targets by appropriately assigning UAVs to attack tasks to already detected targets. Gerkey and Mataric [6] proposed an auction-based task allocation method for multi-robots and showed distributed algorithms are feasible and effective for coordinating multi-robot systems. Sujit and Beard [7] also reported a distributed auction scheme for multiple miniature aerial vehicles, combining it with a greedy strategy. Results show that the distributed task allocation method outperforms a simple greedy technique in terms of time to accomplish a sample mission.

The contribution of this paper is to show the effectiveness of a modified multi-target localization and tracking method for multiple cooperative UAVs, in cases where sensor resources are not sufficient to track each target exclusively, which originated from a multi-target tracking method we reported for a single UAV [8], [9]. The modified method uses a distributed task allocation scheme to influence the decisions made by both the path planner [9] and the sensor manager [8] of each UAV.

The rest of the paper is arranged as follows. In Section II, we give a brief description of coordinate frames used, a camera image projection method, a geo-localization technique, the optimal sensor management technique along with the path planner. We present the modified multi-target tracking algorithm for multiple UAVs in Section III. Analysis of the simulation results of the proposed method is offered in Section IV and we conclude the paper with future research directions in Section V.

II. BACKGROUND

In this section, we briefly describe the relevant coordinate frames used by each UAV, the target state estimation process, an optimal sensor management method [8], and a path planner [9] incorporated in the proposed algorithm to track multiple mobile ground targets using cooperative UAVs.

[1]Authors are with Department of Electrical and Computer Engineering, The University of Texas at San Antonio, San Antonio, Tx 78249, USA. negar.farmani@utsa.edu, liang.sun@utsa.edu,and daniel.pack@utsa.edu.

A. Coordinate Frames and Target Projection

There are four coordinate frames used by UAVs to geo-localize ground targets [10]. The positions of the UAVs and targets are represented in an inertial frame by $\mathbf{p}_u^i = [p_n^i, p_e^i, p_d^i]^T$ and $\mathbf{p}_k^i = [p_{kn}^i, p_{ke}^i, 0]^T$, respectively, where n and e represent the north and east directions, respectively, k denotes the k^{th} target and i defines the inertial frame. The body frame, $F_b \triangleq (i^b, j^b, k^b)$, the gimbal frame, $F_g \triangleq (i^g, j^g, k^g)$, and the camera frame, $F_c \triangleq (i^c, j^c, k^c)$ are three coordinates used to project captured targets in a 3D space onto an image plane. We use rotation matrices, R_b^g and R_g^c which relate the body frame to the gimbal frame and the gimbal frame to the camera frame, respectively, to find $\check{l}_d^b$, the desired gimbal pose in the body frame, given by

$$\check{l}_d^b = \begin{pmatrix} \check{l}_{xd}^b \\ \check{l}_{yd}^b \\ \check{l}_{zd}^b \end{pmatrix} = R_g^b R_c^g \check{l}_d^c. \tag{1}$$

R_g^b is function of the azimuth angle and the elevation angle of the gimbal with respect to the UAV body frame. R_g^c is represented by

$$R_g^c \triangleq \begin{pmatrix} 0 & 1 & 0 \\ 0 & 0 & 1 \\ 1 & 0 & 0 \end{pmatrix}, \tag{2}$$

and $\check{l}_d^c$ is the desired direction of the optical axis which is given by

$$\check{l}_d^c = \frac{\mathbf{l}}{L} = \frac{1}{F} \begin{pmatrix} \varepsilon_x \\ \varepsilon_y \\ f \end{pmatrix}, \tag{3}$$

where ε_x and ε_y are the projected location of target on the image plane, f is the focal length of the camera, $L = ||\mathbf{p}_k - \mathbf{p}_u||$, and F is defined as

$$F \triangleq \sqrt{{\varepsilon_x}^2 + {\varepsilon_y}^2 + f^2}. \tag{4}$$

B. Geo-localization

Each UAV measures its pose in an inertial frame using the Global Positioning System (GPS) signal and an Inertial Measurement Unit (IMU). The position of a target is calculated by performing the image projection transformation, shown as

$$\mathbf{p}_k^i = \mathbf{p}_u^i + L\left(R_b^i R_g^b R_c^g \check{l}_k^c\right), \tag{5}$$

where $\check{l}_k^c$ is the normal vector of target k with respect to the camera frame and

$$R_b^i \triangleq \begin{pmatrix} c_\theta c_\psi & c_\theta s_\psi & -s_\theta \\ s_\phi s_\theta c_\psi - c_\phi s_\psi & s_\phi s_\theta s_\psi + c_\phi c_\psi & s_\phi c_\theta \\ c_\phi s_\theta c_\psi + s_\phi s_\psi & c_\phi s_\theta s_\psi - s_\phi c_\psi & c_\phi c_\theta \end{pmatrix} \tag{6}$$

where $c_\theta \triangleq \cos(\theta)$ and $s_\theta \triangleq \sin(\theta)$. The angels ϕ, θ and ψ are roll, pitch and yaw angles of the UAV, respectively.

We assume the UAV's airspeed, V_a, is constant and the wind speed is zero. The dynamic equation of UAV is given by

$$\begin{pmatrix} \dot{p}_n \\ \dot{p}_e \\ \dot{p}_d \end{pmatrix} = V_a \begin{pmatrix} \cos\psi \\ \sin\psi \\ 0 \end{pmatrix}. \tag{7}$$

The motion model used to estimate the positions and velocities of a target is defined as

$$\dot{x}_i = y_i(x_i, u) + q(t). \tag{8}$$

$x_i = [x_{ni}, x_{ei}, v_{ni}, v_{ei}, L_i]^T$ is the state of target i, where x_{ni}, x_{ei}, v_{ni} and v_{ei} are the i^{th} target's position and velocity in the north and east directions, respectively. L_i is the range between the i^{th} target and the UAV and $y_i = \left(v_{ni}, v_{ei}, 0, 0, \dot{L}_i\right)^T$ is the motion model and $q(t)$ is the associated Gaussian noise.

The prediction step of each target state using the EKF is given by

$$\begin{aligned} \widehat{x}_k &= \widehat{x}_{k-1} + T_s y_i(\widehat{x}_{k-1}, u_k) \\ P_k^- &= P_{k-1}^+ + T_s(A_{k-1}P_{k-1}^+ + P_{k-1}^+ A_{k-1}^T + Q) \end{aligned} \tag{9}$$

where $\widehat{x}$ is the estimated state, $A = \frac{\partial y}{\partial x}(\widehat{x}, u)$ is the system Jacobian matrix, P_k is the state covariance matrix, T_s is the sampling period and $+/-$ superscripts represent after and before measurement updates. Q is the covariance matrix of $q(t)$ and $h(x) = p_k - LR_b^i R_g^b R_c^g \check{l}_d^c$ defines the measurement model. The measurement update of EKF is given by

$$\begin{aligned} C_k &= P_k^- H_k^T (R + H_k P_k^- H_k^T)^{-1} \\ P_k^+ &= (I - C_k H_k) P_k^- \\ \widehat{x}_k &= \widehat{x}_k + C_k(z_k - h(\widehat{x}_k, u_k)), \end{aligned} \tag{10}$$

where $H = \frac{\partial h}{\partial x} = [I \; R_b^i R_g^b R_c^g \check{l}^c]$ is the measurement Jacobian matrix, C is the Kalman gain, R is the sensor covariance, and z is the actual measurement.

C. Optimal Sensor Management - Gimbal Control

An optimal sensor management was proposed in [8] to minimize the overall target location uncertainties. A dynamic weighted graph method was used to determine the sensor gimbal pose. A graph, $G \triangleq [g_{ij}] \in \Re^{n \times n}$, represents the distance relations among targets. Each element of matrix G is given by

$$g_{ij} = \begin{cases} 0 & \text{if } i = j \\ \frac{e^{-|d_{ij}|}}{\sqrt{(\delta_{x_i} + \delta_{x_j})^2 + (\delta_{y_i} + \delta_{y_j})^2}}, & \text{if } i \neq j \end{cases} \tag{11}$$

where d_{ij} is the estimated distance between targets i and j, δ_{x_i}, δ_{x_j}, δ_{y_i} and δ_{y_j} are estimated position variances of targets i and j in the north and east directions, respectively.

The numerator of (11), when $i \neq j$, awards targets that are close to each other. The denominator incorporates the uncertainties of position estimations of both targets i and j. The resulting matrix, G, is a weighted symmetric matrix based on estimated distances among targets. The summation of i^{th} column of matrix G represents the density of targets near target i. It shows the larger the summation the greater number of the other targets close to target i. We select n largest summations, corresponding n regions with high target densities, as the gimbaled camera pose candidates and apply sensor constraints to each candidate to determine the number of targets in the field of view (FOV). To find the final gimbal pose, we apply a Model Predictive Control

(MPC) technique to evaluate the overall uncertainties of the captured targets in the FOV. The MPC function is given by (12), which incorporates the information matrix, P_i^{-1}, and the information gain obtained by the UAV, $H^T R^{-1} H$, for target i.

$$\begin{aligned} &\text{minimize} \prod_{i=1}^{n} tr(P_i^{-1} + a_i H^T R^{-1} H)^{-1} \\ &\sum_{i=1}^{n_{FOV}} a_i = \text{number of targets in FOV}, \end{aligned} \tag{12}$$

$a_i \in \{0,1\}$ and n_{FOV} is the number of targets within the FOV. The trace of resulting matrix in (12) captures the overall covariance of all targets and the multiplication operator is used to amplify the difference between gimbal pose candidates. The candidate with the minimum cost of (12) is selected as the optimal gimbal pose.

D. Path Planner

An optimal real-time path planner for a single UAV considers two time horizon steps of the UAV path as shown in Fig. 1. The cost function shown in (13) incorporates the uncertainty of state estimation and distance among the UAV and targets:

$$\text{maximize} \sum_{i=0}^{n_t} f\left(P_i, d_{i,i+1}, \frac{dP_i}{dt}\right), \tag{13}$$

where P_i is the covariance of target i, $d_{i,i+1}$ is the distance between target i and $i+1$, and $\frac{dP_i}{dt}$ represents the derivative of the covariance of target i. n_t defines the number of targets and the UAV is denoted as the 0^{th} target, where $P_0 = \frac{dP_0}{dt} = 0$. Equation (13) is the sum of two time step costs. Each cost is used for a time horizon step of the UAV path. The first cost function, which is given in (14), incorporates the uncertainty of target i, distance of the UAV from target i, and the time integral of the time derivative of target i's covariance matrix in the north and east directions. The integral is over the estimated time for the UAV to reach target i.

$$f_1(P_i, d_{ui}, \frac{dP_i}{dt}) = w_1|P_i| + w_2\frac{1}{d_{ui}} + w_3(\int_0^{t_{ui}} \dot{P}_{ix}(t)\dot{P}_{iy}(t)dt). \tag{14}$$

In (14), $|P_i|$ is the determinant of the covariance matrix of target i and indicates that the target with a larger uncertainty will have a bigger influence toward the cost. The term, $\frac{1}{d_{ui}}$, the inverse of the distance between the UAV and the i^{th} target, indicates that a target which is closer to the UAV should contribute more to the cost than the one farther away. The last term in (14) incorporates the rates of change of position uncertainties of target i in the north and east directions, respectively. The traveled time for UAV to reach target i is given by

$$t_{ui} = \frac{d_{ui}}{V_a}. \tag{15}$$

The weights, w_1, w_2 and w_3 are chosen based on the importance of each term. We normalize each term in (14) to select appropriate weights.

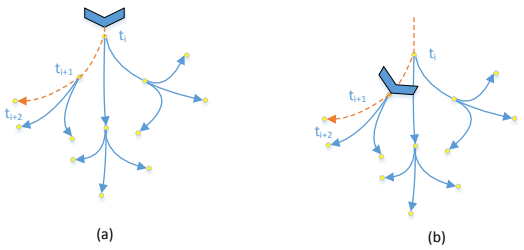

Fig. 1. Two time horizon step used by a UAV path planner: a) UAV at the start of the first time step, and b) UAV at the start of second time step.

The cost function for the second time horizon step considers the travel cost for the UAV to move from target i to the next target.

$$f_2\left(P_j, d_{ij}, \frac{dP_j}{dt}\right) = e^{-\beta t_{uj}}\left(w_1|P_j| + w_2\frac{1}{d_{ij}} + w_3\int_0^{t_{uj}} \dot{P}_{jx}(t)\dot{P}_{jy}(t)dt\right). \tag{16}$$

The term, $\frac{1}{d_{ij}}$, is the inverse of the distance between targets i and j which shows the cost involved for the UAV to reach target j after reaching target i. The integral of derivatives of the position covariances is taken over the travel time of the UAV to reach target j after it reaches target i, and the travel time is calculated as

$$t_{uj} = \frac{d_{ui} + d_{ij}}{V_a}. \tag{17}$$

Weights are calculated the same way as before and the exponential term at the start of the cost function reflects the needed decreasing value of the cost based on time delay of the UAV to reach target j with user a specified parameter, β. The maximum sum of two cost functions in (14) and (16) determines the optimal UAV path, i.e., the straight line to one of the targets. The process is repeated as the covariance matrix gets updated.

III. A MULTI-TARGET TRACKING METHOD FOR MULTIPLE COOPERATIVE UAVS

A distributed target tracking method for multiple cooperative UAVs is presented in this section. We use the overall target position estimation uncertainties as our success criteria. Consider n UAVs, equipped with communication modules and gimbaled camera sensors, tracking multiple mobile ground targets. Suppose also the number of UAVs is less than the number of targets. For each UAV, targets are captured using a gimbaled cameras, after the UAV's location and the gimbal sensor pose are determined by the sensor management technique and the path planner described in Section II. Once captured, each target location and velocity are estimated using the EKF, also described in Section II.

Due to limited FOV and the camera sensing range, it is essential that UAVs work cooperatively, since it is not

possible for the UAVs to individually track all targets and update their states. The proposed algorithm residing on each UAV combines the target estimates of all participating UAVs together and determines its path and gimbaled sensor pose. The algorithm contains two parts: a cooperative path planner and a conflict-free, cooperative gimbal pose controller.

We describe the proposed algorithm using three sub-algorithms. Once target estimates are computed or received from other neighboring UAVs, a combined covariance matrix, P, representing the current knowledge about targets for the UAV is selected. As Algorithm 1 shows, for each target, the determinant of state covariance matrix, P_{ij}, is calculated, where i and j are the indexes of a target and a UAV, respectively, where NoT is the number of targets and NoU is the number of UAVs. P_{ij} represents the knowledge of the j^{th} UAV of target i. We use the determinant as the amount of estimation uncertainty. Each UAV then compares its knowledge of target i with other UAVs and finds the minimum P_{ij} as the best estimation of the i^{th} target. Once

Algorithm 1 Decentralized data fusion for individual UAV

```
for i=1:NoT do
    for j=1:NoU do
        PP(j) = |P_ij|
    end for
    P_fuse(i) = min(PP)
end for
```

the optimal covariance of each target is determined, the cost function, (13), is used to calculate the UAV path. Algorithm 2 is used to de-conflict UAV paths for cases where same targets are selected by multiple UAVs, using an auction method. The procedure is repeated as necessary until all UAVs find different flight paths.

Algorithm 2 UAV path task assignment for individual UAV

```
For each UAV(UAV_i)
while UAV_i plans to fly to the same target as UAV_j do
    if maxCostUAV_i > maxCostUAV_j then
        Assign UAV_i to fly to the selected target
    else
        Find a target with the next maximum cost value
        End the While loop
    end if
end while
```

Once different paths of the UAVs are determined, the cost function in (12) is used to assign a gimbaled camera pose for each UAV. The third algorithm, Algorithm 3, is used for cases when cameras onboard UAVs are pointing to a same target or targets. Algorithm 3 shows the conflict-free process for UAVs where d_k defines the distances from UAV k to the same target. The UAVs share their gimbal poses and each UAV compares targets being captured by its gimbal pose with those of other UAVs. If two UAVs decide to point their gimbal poses to capture the same target, the UAV which is closer in distance to that target has the priority, reflecting the limitation of camera sensing range. The other UAV chooses the next best target for its gimbal pose. If the distance between UAVs and selected target is equal, then the UAV with the lower gimbal pointing cost wins that selection. This process is repeated, if necessary. Fig. 2 shows the block diagram of the proposed method for each UAV. To reduce the amount of communicated data and computation with a large number of UAVs, one can devise a method that only shares the gimbal information with its neighboring UAVs. We understand that the computational complexity of the algorithms will increase exponentially as the number of the UAVs increases. By limiting the number of neighbors, we can manage the amount of computations needed for each UAV, which we plan to do in the future.

Algorithm 3 Gimbal task conflict-free for individual UAV

```
For UAV_i
while gimbal of UAV_i points to the same target as UAV_j do
    d_i = distance between UAV_i and target
    d_j = distance between UAV_j and target
    if d_i < d_j then
        Point the gimbal to the target
    else
        Find the next gimbal pose candidate
    end if
end while
```

IV. SIMULATION RESULTS

In this section, we present simulation results to show the effectiveness of the proposed multi-target localization and tracking method for cooperative UAVs. Each UAV operates with a path planner and a sensor manager using the cost functions and the procedures described in Section II and Section III. We first show the performance improvement resulted from applying the proposed algorithm to two UAVs tracking five mobile targets against the one using the same system that does not share any data between the two UAVs. UAVs fly at a constant altitude 100 m above the ground with the speed of 13 m/s. The camera onboard each UAV has a maximum range of 250 m and the GOV of 40 degrees. The target movements are random and piecewise linear with the speed of 5 m/s in an urban environment. We ran the experiment 100 times, each lasting for 100 seconds. The initial positions of targets and UAVs were assigned randomly for each run but they were identical for both methods: Method 1 represents the system working independently and Method 2 the system working cooperatively. We assume that once a gimbaled pose is determined, it is fixed two seconds before it can be changed again.

Fig. 3 shows the simulation environment within which the UAVs and targets operate. The small blocks represent buildings and the lines are roads in a city. Fig. 4 represents the five target trajectories and the two UAVs' paths for a sample experiment run.

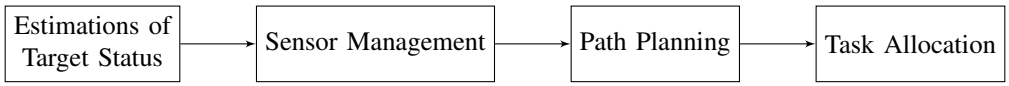

Fig. 2. Block diagram of the presented algorithm for each UAV.

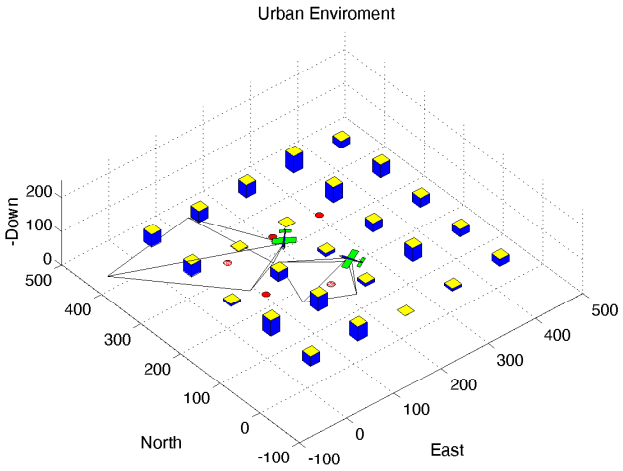

Fig. 3. Simulation environment.

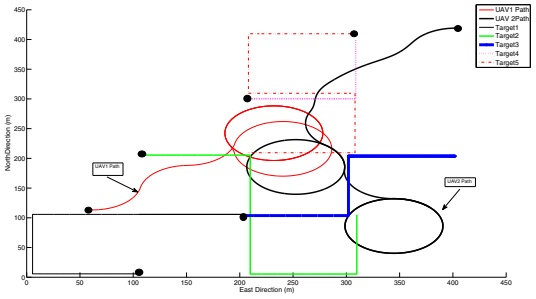

Fig. 4. Trajectories of targets and UAVs. The dots show the starting points for five targets and two UAV trajectories.

Fig. 5 shows the average summation of location errors for the five targets in the north and east directions, respectively, using Method 1(solid line) and Method 2 (dashed line). As expected, there is a significant performance improvement when the two UAVs cooperate by sharing target estimates, planned trajectories, and gimbal poses.

Table I shows the estimation errors for individual targets using both methods while Table II shows the overall position estimation errors of five targets over 100 runs. The numerical results and the percentage of performance difference show the effectiveness of the proposed algorithm.

To find out how the data sharing between UAVs improved the overall performance, we recorded the number of times the two UAVs had to resolve conflicts (heading toward or pointing their gimbals to the same target) during each run.

Fig. 6 shows a sample histogram of incidents when two UAVs determined to point their sensors toward the same target during a single run. The horizontal axis shows the target number and the vertical axis shows the number of times one particular target was chosen by both UAVs. Last column in the figure represents cases when the same two or more targets were chosen by the UAVs. Each UAV makes the gimbal pose decision every 2 seconds.

Fig. 7 shows the number of cases when both UAVs planned to fly toward the same target. Again, the horizontal axis shows the target number while the vertical axis shows the number of times both UAVs decided to fly to the same target. Each UAV regenerates its path to a target every 0.1 second.

The experiments show that 70 percent of the time, the two

TABLE I
AVERAGE TARGET GEO-LOCATION ERRORS(FIVE TARGETS) IN THE NORTH AND EAST DIRECTIONS BASED ON 100 EXPERIMENTS USING METHOD 1 (M1) AND METHOD 2 (M2).

Target No.	1	2	3	4	5
Error in Pos(N) (m) (M1)	50.53	84.56	55.13	33.68	31.24
Error in Pos(N) (m) (M2)	9.98	3.26	17.38	15.49	12.65
Error in Pos(E) (m) (M1)	116.7	84.13	60.47	20.44	34.02
Error in Pos(E) (m) (M2)	11.94	6.78	16.55	16.43	12.22

TABLE II
AVERAGE TOTAL TARGET GEO-LOCATION ERRORS IN THE NORTH AND EAST DIRECTIONS USING METHOD 1 (M1) AND METHOD 2 (M2).

Overall Error	Error	Difference (%)
Average total North Position Error (m) (M1)	51.02	
Average total North Position Error (m) (M2)	12.65	75.2
Average total East Position Error (m) (M1)	63.01	
Average total East Position Error (m) (M2)	12.78	79.7

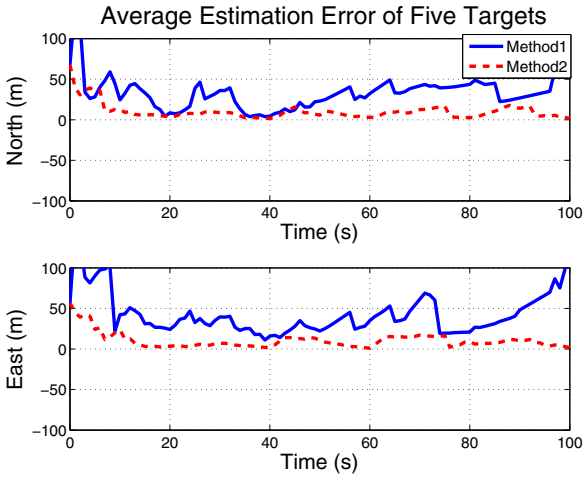

Fig. 5. Average of five target geo-location errors resulted from running Method 1 and Method 2 for a sample experimental run.

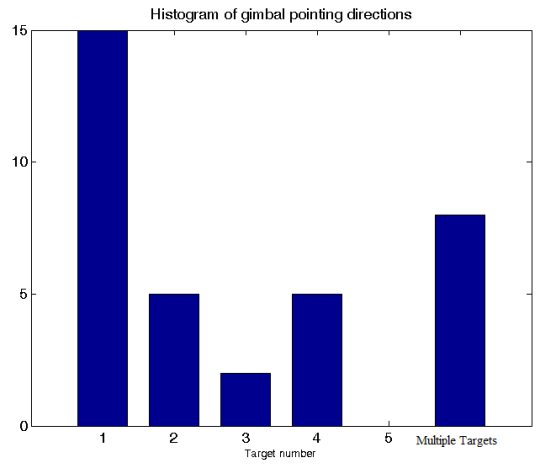

Fig. 6. Gimbal pose conflict histogram.

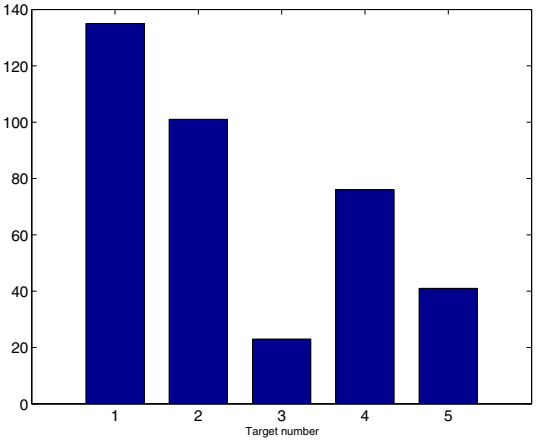

Fig. 7. Path conflict histogram of UAVs.

UAVs had to resolve the gimbal poses and negotiate for path solutions for 37 percent of the time. The target estimates, planned paths, and gimbal poses were shared between UAVs every 0.1 second, 0.1 second, and 2 seconds, respectively. The data show for a typical tracking scenario, a significant amount of work is duplicated by UAVs. We plan to perform analysis study that shows the system performance depending on type and frequency of data shared between UAVs.

V. CONCLUSIONS

In this paper, we proposed and demonstrated a new multi-target localization and tracking algorithm for multiple UAVs. The distributed algorithm takes advantage of sharing of data amongst path planners and sensor managers onboard UAVs. The decentralized method showed significant performance improvement when compared with similar systems without data sharing, showing the quantifiable benefits of using a cooperative approach in tracking multiple targets. For future research, we plan to study the effect of the proposed method as we increase the number of UAVs and targets. We also plan to perform analysis with varying sensor and communication parameters.

REFERENCES

[1] G. Chen and J. B. Cruz Jr, "Genetic algorithm for task allocation in uav cooperative control," in *AIAA Conference on Guidance, Navigation, and Control*, 2003.

[2] L. F. Bertuccelli, H.-L. Choi, P. Cho, and J. P. How, "Real-time multi-uav task assignment in dynamic and uncertain environments," in *presentado al AIAA Guidance, Navigation, and Control Conference, Chicago, Illinois*, 2009.

[3] M. A. Darrah, W. M. Niland, and B. M. Stolarik, "Multiple uav dynamic task allocation using mixed integer linear programming in a sead mission," *Infotech@ Aerospace*, pp. 26–29, 2005.

[4] P. Sujit, A. Sinha, and D. Ghose, "Multiple uav task allocation using negotiation," in *Proceedings of the Fifth International Joint Conference on Autonomous Agents and Multiagent Systems*. ACM, 2006, pp. 471–478.

[5] M.-H. Kim, H. Baik, and S. Lee, "Response threshold model based uav search planning and task allocation," *Journal of Intelligent & Robotic Systems*, pp. 1–16, 2013.

[6] B. Gerkey and M. Mataric, "Sold!: auction methods for multirobot coordination," *Robotics and Automation, IEEE Transactions on*, vol. 18, no. 5, pp. 758–768, Oct 2002.

[7] P. Sujit and R. Beard, "Multiple mav task allocation using distributed auctions," in *AIAA Guidance, Navigation and Control Conference and Exhibit*, 2007, pp. 20–23.

[8] N. Farmani, L. Sun, and D. Pack, "An optimal sensor management technique for unmanned aerial vehicles tracking multiple mobile ground targets," in *Unmanned Aircraft Systems (ICUAS), 2014 International Conference on*, May 2014, pp. 570–576.

[9] N. Farmani, L.Sun, and D. Pack, "Optimal uav sensor management and path planning for tracking multiple mobile targets," in *ASME 2014 Dynamic Systems and Control Conference*. American Society of Mechanical Engineers, 2014, pp. V002T25A003–V002T25A003.

[10] R. Beard and W. McLainTimothy, *Small Unmanned Aircraft: Theory and Practice*. Princeton University Press, 2012.